

# Effect of cooling rate on the formation of metastable icosahedral quasicrystal phase in rapidly solidified Al–8.2at% Mn alloy

TIANYI CHENG\*, SHOUHUA ZHANG†

\*Metal Materials Section, Department of Mechanical Engineering, Beijing Institute of Technology, P.O. Box 327, Beijing 100081, China

†Faculty of Materials Science and Engineering, University of Science and Technology, Beijing, Beijing, China

The microstructure of rapidly solidified Al–8.2at% Mn alloy was analysed by X-ray diffraction, transmission electron microscopy and energy-dispersive analysis of X-rays and the effect of cooling rate on the formation of the metastable icosahedral quasicrystal phase (IQP) was investigated. The formation of IQP was found to be sensitive to the cooling rate in a rapidly solidified alloy of a certain composition. A lower critical cooling rate at which metastable IQP starts to appear and an upper critical cooling rate at which IQP suppresses completely the stable crystalline phase exist. The fact that the amount and the manganese concentration of IQP change non-linearly with the cooling rate suggests that there is an optimum cooling rate at which both the amount of IQP and its solute concentration reach maximum values in an alloy of a certain composition.

## 1. Introduction

Since Shechtman *et al.* [1] discovered the icosahedral quasicrystal phase (IQP) in rapidly solidified Al–Mn (18 to 25.3 wt% Mn), Al–Cr and Al–Fe alloys, the novel phase, which has a icosahedral point-group symmetry that crystals cannot possess and a long-range orientational order, has attracted intense interest [2–5]. The mechanism of the formation of IQP is an interesting and important aspect, and the effect of the nominal composition of an alloy on the formation of IQP has been investigated [3, 6]. However, a number of works [7–10] indicated that IQP in Al–Mn alloys would transform into the equilibrium phase  $Al_4Mn$  or  $Al_6Mn$  after properly heating, even for those IQP which formed not during rapid solidification but during precipitation [9]. These facts suggest that IQP is a metastable phase and its formation is dominated mainly by kinetic factors, not by thermodynamic ones [21]. It seems that the cooling rate is the most important and relatively easy to control kinetic parameter although the cooling rate is related to the formation of IQP through the solidification rate. Therefore, exploration of the effect of cooling rate on the formation of IQP is not only helpful in understanding the mechanism of its formation and the formation of the other metastable phases, but also useful in preparing pure IQP to open a possible way for utilizing them in practice. However, up to now little research in this aspect has been published.

In this work, the microstructures of cast and rapidly solidified Al–8.2at% Mn alloy were studied and the effect of the cooling rate with the formation of metastable IQP was explored.

## 2. Experimental procedure

Al–8.2at% Mn cast alloy was prepared with pure aluminium (99.99 mass%) and manganese (99.9 mass%) by melting in an argon atmosphere. Then the cast alloy was spun into ribbons by melt spinning using a copper wheel (34 cm diameter) as chill substrate. The ribbons thus obtained were generally 4 mm wide. Three wheel peripheral velocities,  $v$ , were selected to vary the ribbon thickness. The average ribbon thickness,  $d$ , was measured on the cross-section of the ribbon by SEM. The evaluation of the cooling rate in rapidly solidified alloys is very difficult and to date there has been no method in which the cooling rate can be measured or calculated accurately [10], especially when the morphology of IQP exhibits a non-traditional dendritic form. This may be why the cooling rate was not reported in most papers related to IQP. However, the cooling rate was found to be a function of the ribbon thickness [11, 12], so using an empirical relation between the cooling rate and the mean thickness of ribbons [13, 14], which is independent of the kind of solid phase, the corresponding average cooling rates in ribbons were calculated.

\* Present address: Department of Materials, University of Oxford, Parks Road, Oxford OX13PH, UK.

TABLE I Wheel peripheral speed,  $v$ , ribbon thickness,  $d$ , and cooling rate,  $\dot{T}$ , of spun ribbons

Ribbons	$v$ (m sec <sup>-1</sup> )	$d$ ( $\mu$ m)	$\dot{T}$ (10 <sup>6</sup> K sec <sup>-1</sup> )
B-1	32.0	12.8	3.0
B-2	26.7	16.2	2.4
B-3	17.8	23.2	1.7

These results are summarized in Table I. The calculated values of cooling rates are very close to those reported by Dunlap and Dili [15] who discovered IQP in rapidly solidified Al-V alloy; the thickness of their ribbons was nearly the same as that of ribbons studied in our experiment.

X-ray diffraction was performed with a Philips PW 1700 X-ray diffractometer using CuK $\alpha$  radiation on the broad face of ribbons pasted on to a glass plate by means of an amorphous glue. The microstructures of rapidly solidified alloy were studied with EM-400T and H-700 electron microscopes. Foils for TEM were prepared by electrolytic polishing using a twin jet in an electrolyte of perchloric acid and alcohol 1:9 by volume. The microchemistry of the constituent elements was determined by energy-dispersive analysis of X-rays together with TEM. Because it is known that the structure along a ribbon changes owing to variation in cooling rate, prior to study in the X-ray diffractometer and TEM all ribbons were worn away slightly from the wheel side and free side, respectively, so that the middle zone of a ribbon was analysed, thus the cooling rate was close to the average cooling rate of a ribbon.

### 3. Results

#### 3.1. Analysis of phase constitution

An X-ray diffraction pattern for the as-cast alloy is shown in Fig. 1. ASTM cards were used in the identification of the pattern. The alloy consists of  $\alpha$ -Al and Al<sub>6</sub>Mn phases as shown in Fig. 1. Fig. 2 shows a portion of the Al-Mn equilibrium phase diagram [16]. It can be deduced that solidification in the as-cast alloy is very close to equilibrium solidification and  $\alpha$ -Al and Al<sub>6</sub>Mn phases are the stable phases in Al-8.2 at % Mn alloy.

X-ray diffraction patterns of spun ribbons are given in Fig. 3. ASTM cards and previous work [2, 17, 18] were used in the identification of the patterns. It can be

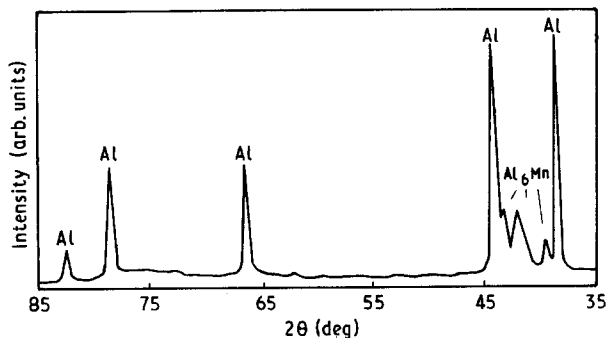


Figure 1 X-ray diffraction pattern of as-cast Al-8.2Mn alloy.

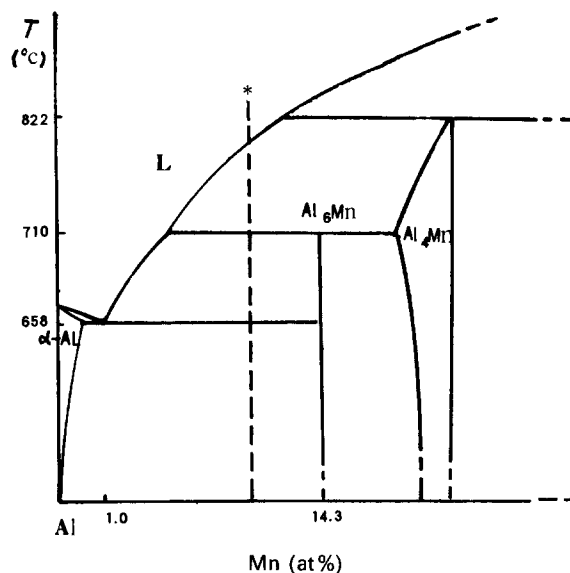


Figure 2 A portion of the Al-Mn phase diagram. (\*) Al-8.2Mn alloy.

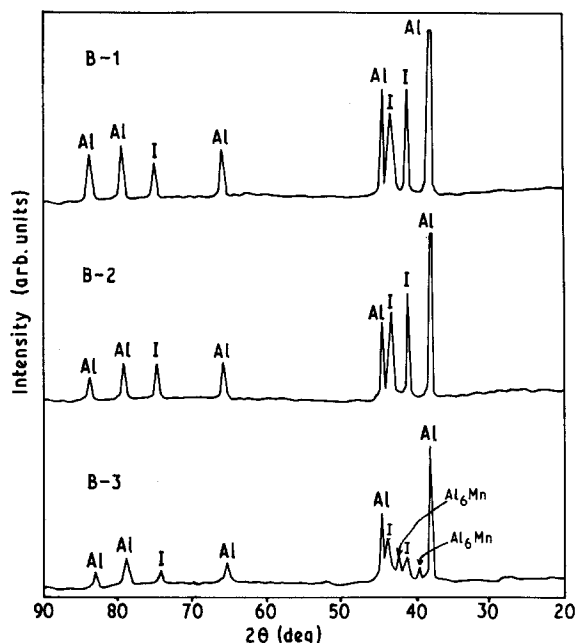


Figure 3 X-ray diffraction patterns of spun ribbons.

seen that the stable Al<sub>6</sub>Mn phase was replaced completely by the metastable IQP in ribbons B-1 and B-2, but only partly in ribbon B-3.

#### 3.2. Measurement of lattice parameter of $\alpha$ -Al

The lattice parameters,  $a$ , for as-cast and spun alloy were measured by X-ray diffraction using a traditional method [19] (see Table II). It can be seen that the

TABLE II Lattice parameter,  $a$ , of  $\alpha$ -Al for as-cast and as-spun alloy

	As-spun alloy			
	As-cast alloy	Spun ribbons		
		B-1	B-2	B-3
$a$ (nm)	0.405 10	0.404 08	0.404 37	0.403 20

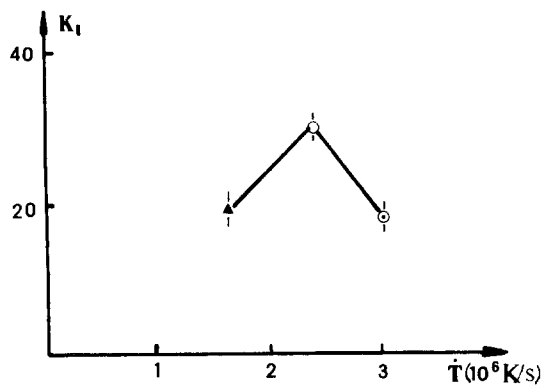


Figure 4 Relation between ratio of peak intensities of IQP (1 0 0 0 0) reflection to  $\alpha$ -Al (1 1 1) reflection  $K_1$ , and the cooling rate  $\dot{T}$ . (○) B-1, (○) B-2, (▲) B-3.

lattice parameter of  $\alpha$ -Al in as-cast alloy is very close to the equilibrium value 0.405 06 nm [20] and those in spun alloy are smaller. Because the atomic diameter of manganese is smaller than that of aluminium it suggests that  $\alpha$ -Al in the spun alloy is the metastable supersaturated solid solution. It is noted that the lattice parameter of  $\alpha$ -Al in B-2 is the largest among the spun ribbons.

### 3.3. The relation between the amount of IQP and the cooling rate

Because the diffraction intensity of one phase is directly proportional to its content in a two-phase alloy [19], IQP and  $\alpha$ -Al phases are the principal constituents in these ribbons, except for a small amount of  $\text{Al}_6\text{Mn}$  phase present in B-3. From the work of Inoue *et al.* [3], a parameter  $K_1 = (100000)_{\text{IQP}} / (111)_{\alpha\text{-Al}}$ , may be defined as the ratio of heights of the main X-ray diffraction peaks of IQP and  $\alpha$ -Al. The magnitude of the parameter  $K_1$  indicates the relative amount of IQP in a specimen approximately. Fig. 4 shows the parameter  $K_1$  as a function of the cooling rate and it can be seen that the amount of IQP is the largest in ribbon B-2 when  $\dot{T} = 2.4 \times 10^6 \text{ K sec}^{-1}$ .

### 3.4. Microstructures

Microstructures of ribbon B-1 are given in Fig. 5. The matrix phase is the  $\alpha$ -Al phase and the second is IQP. Most IQP have a typical morphology of radial dendrites or spherulites instead of the traditional crystalline dendrites [21]. From the morphologies and distribution of IQP and  $\alpha$ -Al it is seen that the solidification of  $\alpha$ -Al occurred after the formation of IQP [22]. Fig. 6 shows selected-area electron diffraction patterns (SAED) for IQP and  $\alpha$ -Al in ribbon B-1. Microstructures and SAED patterns for ribbons B-2 and B-3 are shown in Fig. 7. It is seen that the dendritic grains of IQP in these ribbons became coarse and well developed. A few small grains of  $\text{Al}_6\text{Mn}$  appeared among the IQP dendrites in the  $\alpha$ -Al matrix of B-3 (see Figs 7c and d). Obviously, the microstructures of the spun alloy are in good accord with the X-ray diffraction results.

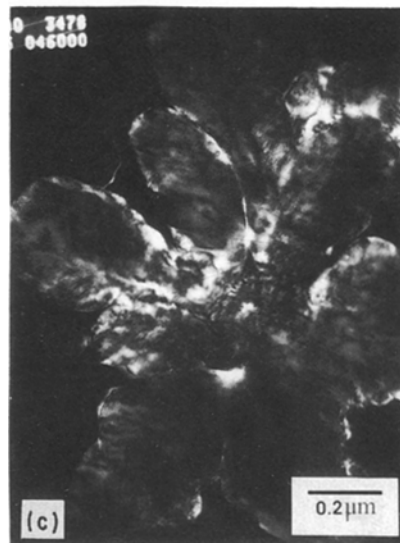
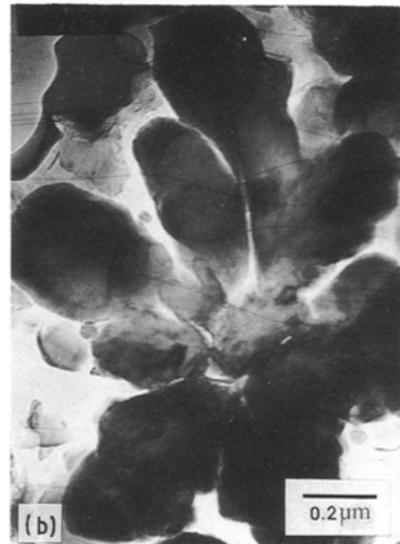
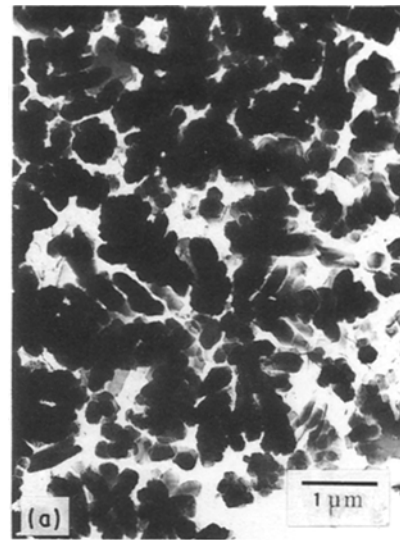


Figure 5 TEM microstructures in ribbon B-1: (a)  $\alpha$ -Al matrix phase and IQP; (b) dendrite of IQP; (c) dark-field micrograph corresponding to (b).

### 3.5. Microchemical analysis

Fig. 8 shows the dependence of manganese content in IQP and  $\alpha$ -Al measured by EDX, on the cooling rates in the spun alloy. The manganese concentration of

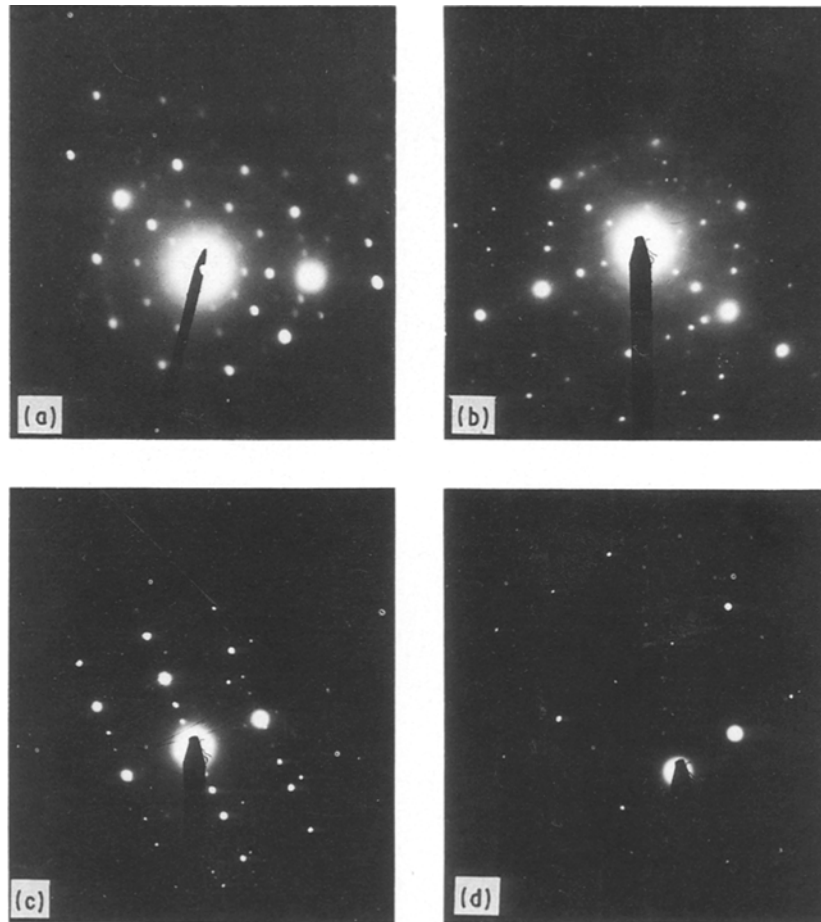


Figure 6 SAED patterns of B-1 ribbon: (a) to (c) diffractions of IQP; (d) diffraction of  $\alpha$ -Al, [1 1 2] zone.

IQP has a maximum value and that of  $\alpha$ -Al has a minimum value in spun ribbon B-2.

#### 4. Discussion

Samuel *et al.* [2] discovered IQP in their rapidly solidified ribbons spun with different wheel peripheral speeds in Al-15 wt % (8 at %) Mn alloy, but no  $\text{Al}_6\text{Mn}$  was found. Shechtman *et al.* [23] investigated Al-Mn alloy of the same composition before discovering IQP in other experiments [1], but they observed only crystalline phases. These contradictory results can be easily explained by comparing their findings with our results pertaining to the dependence of the formation of IQP on the cooling rate. It is noted that the compositions of alloys used in their experiments are nearly the same as ours. Shechtman *et al.*'s ribbon is 40  $\mu\text{m}$ , which is thicker than our ribbon B-3, thus the cooling rate in their ribbon must be smaller than that of B-3, i.e. smaller than  $1.7 \times 10^6 \text{ K sec}^{-1}$ . On the other hand, Samuel used a ribbon of 20 to 30  $\mu\text{m}$  which is thinner than that of Shechtman *et al.*, but thicker than our ribbon B-2. Thus the cooling rate in Samuel's ribbon is higher than Shechtman *et al.*'s, but is lower than in ribbon B-2. Therefore, it is easy to understand why Samuel observed IQP while Shechtman did not in alloys of similar composition. It is evident that the formation of IQP is sensitive to the cooling rate in a rapidly solidified alloy. In Al-Mn alloys the cooling rate at which IQP starts to form

should be about  $10^6 \text{ K sec}^{-1}$  which is the same as estimated by Schaefer *et al.* [22] and Shechtman [24]. Accordingly, a lower critical cooling rate  $\dot{T}_{C2}$ , equal to about  $10^6 \text{ K sec}^{-1}$  in Al-8 at % Mn alloy, can be defined, at which the metastable IQP starts to form.

Our investigation has suggested that the formation of the metastable IQP is the result of the competition of nucleation between IQP and another stable phase, which is  $\text{Al}_6\text{Mn}$  phase in Al-8 at % Mn alloy. In such a competition the cooling rate plays a very important role. Metastable IQP suppresses completely the stable  $\text{Al}_6\text{Mn}$  phase in ribbons B-1 and B-2 when the cooling rate  $\dot{T} \geq 2.4 \times 10^6 \text{ K sec}^{-1}$ , but replaces it only partly in ribbon B-3 when  $\dot{T} = 1.7 \times 10^6 \text{ K sec}^{-1}$ . This implies that there is an upper critical cooling rate  $\dot{T}_{C1}$ . When  $\dot{T} \geq \dot{T}_{C1}$  in an alloy with a certain composition the metastable phase suppresses completely the competing stable phase. In Al-8.2 at % Mn alloy,  $\dot{T}_{C1} \sim 2.4 \times 10^6 \text{ K sec}^{-1}$ . A similar result was obtained in rapidly solidified Ni-Al alloys [25].

Obviously, exploring these phenomena is very important in predicting and controlling the formation of IQP or other metastable phases. Based on the thermodynamics and competitive nucleation kinetics we analysed the mechanism of formation of metastable phase during rapid solidification and presented a criterion that the metastable phase suppresses completely the stable one, and a method for calculating the corresponding upper critical cooling rate,  $\dot{T}_{C1}$  [26]. The

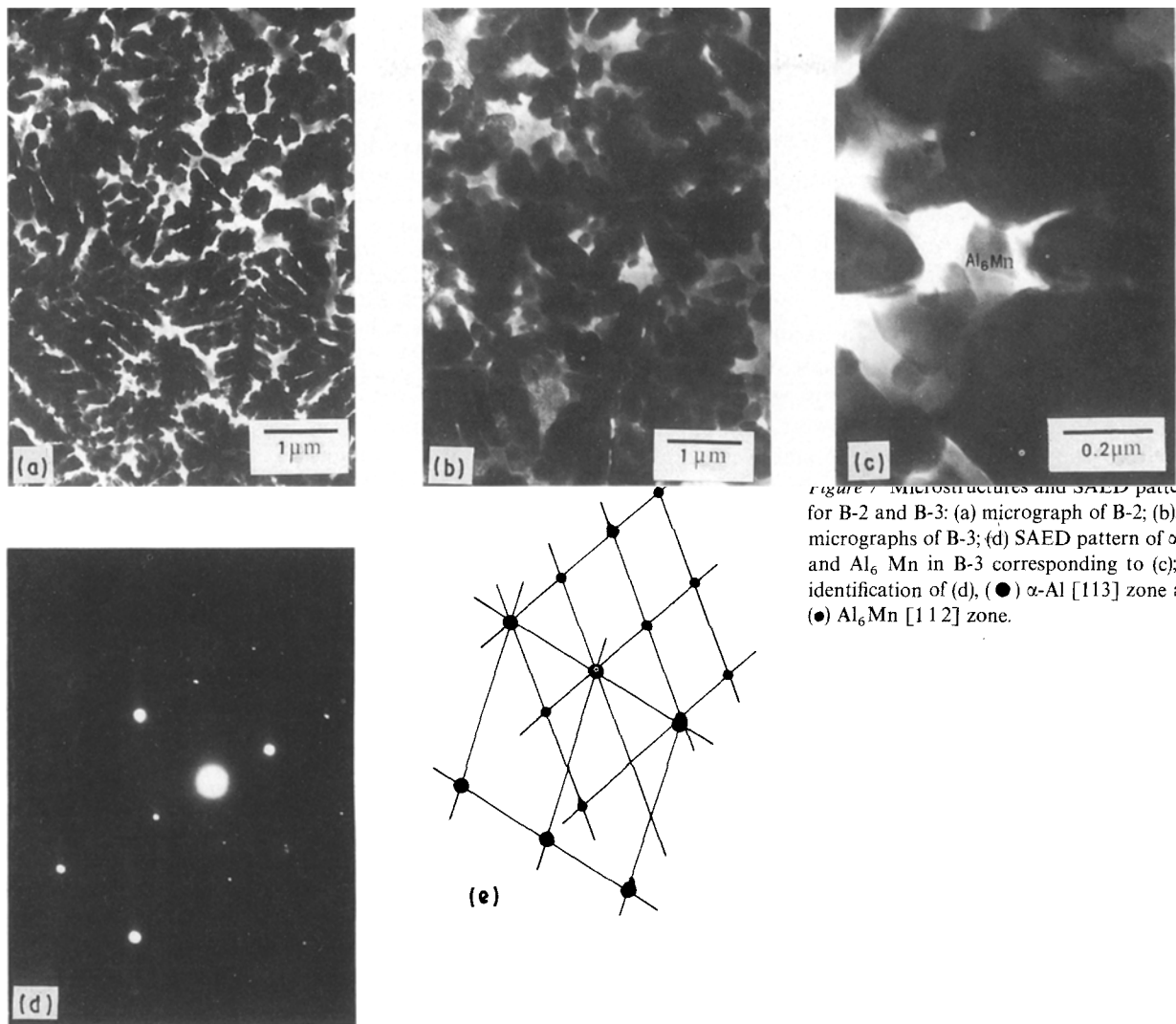


Figure 7. Microstructures and SAED patterns for B-2 and B-3: (a) micrograph of B-2; (b), (c) micrographs of B-3; (d) SAED pattern of  $\alpha$ -Al and  $\text{Al}_6\text{Mn}$  in B-3 corresponding to (c); (e) identification of (d), (●)  $\alpha$ -Al [113] zone and (●)  $\text{Al}_6\text{Mn}$  [1 1 2] zone.

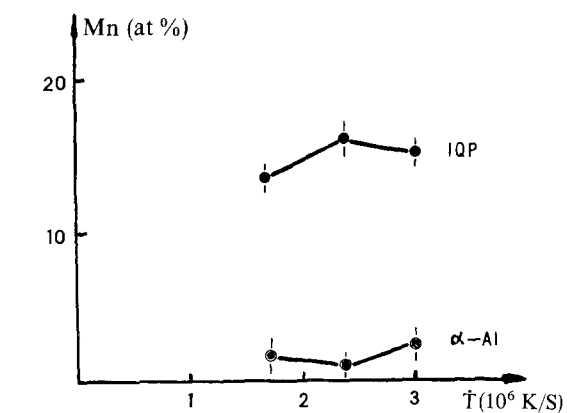


Figure 8. Dependence of manganese concentrations in IQP and  $\alpha$ -Al on cooling rates in spun ribbons.

calculated value is in good accord with the experimental results in Ni-Al alloy. However, because the values of some kinetic parameters in Al-Mn alloys, such as the energy of the solid-liquid interface  $\sigma_{\text{SL}}$ , were not available, calculation of  $\dot{T}_{\text{C1}}$  for IQP cannot yet be made but a qualitative deduction based on our theoretical work suggests that  $\sigma_{\text{SL}}$  of the metastable IQP must be smaller than that of competing stable

$\text{Al}_6\text{Mn}$  phase, which agrees with other results [27]. Evidently, further study on this aspect is needed.

Finally, as observed above, in our Al-8.2 at % Mn alloy the amount and composition of IQP changes non-linearly with cooling rates and at a cooling rate  $\dot{T} = 2.4 \times 10^6 \text{ K sec}^{-1}$  both the amount and the manganese concentration of IQP attain their maximum values. The maximum manganese concentration (16.3 at % Mn) is close to the stoichiometric value of IQP in Al-Mn alloys ( $\text{Al}_4\text{Mn}$  as suggested by Inoue [3]). Accordingly, it seems that for rapidly solidified Al-Mn alloys of a definite composition there is an optimum cooling rate,  $\dot{T}_0$ , at which both the amount of IQP and its manganese concentration reach their maximum possible values. In fact Sastry [28], based on his experiments in rapidly solidified Mg-Cu-Al alloy, made the conjecture that there would be an optimum cooling rate for the formation of IQP. It is further speculated that the dependence of the  $\sigma_{\text{SL}}$  of IQP on the cooling rate is non-linear, and when  $\dot{T} = \dot{T}_0$  the  $\sigma_{\text{SL}}$  of IQP is the smallest, so that IQP is the most easily formed. Obviously, it is possible that lower and upper critical cooling rates and the optimum cooling rate also apply for other metastable phases in rapidly solidified alloys with a certain composition.

We believe that further exploration of this aspect is required.

## 5. Conclusions

1. The formation of IQP is sensitive to the cooling rate in a rapidly solidified alloy and there is a lower critical cooling rate,  $\dot{T}_{C2}$ , which is the lowest cooling rate for IQP to appear. In Al-8.2 at % Mn alloy,  $\dot{T}_{C2}$  is  $\sim 10^6$  K sec<sup>-1</sup>.

2. The formation of IQP is the result of its competition with the stable crystalline phase, which is Al<sub>6</sub>Mn in Al-8.2 at % Mn alloy. There is an upper critical cooling rate,  $\dot{T}_{C1}$ , which is the lowest cooling rate for IQP to suppress completely the stable phase in an alloy with a certain composition. In Al-8.2 at % Mn alloy,  $\dot{T}_{C1}$  is  $\sim 2.4 \times 10^6$  K sec<sup>-1</sup>.

3. The amount and solute concentration of IQP change non-linearly with cooling rate. In Al-8.2 at % Mn alloy, the manganese concentration varies from 13.7 to 16.3 at % when  $\dot{T} = 1.3 \times 10^6$  to  $\sim 3.0 \times 10^6$  K sec<sup>-1</sup>. It is possible that an optimum cooling rate,  $\dot{T}_0$ , exists at which both the amount of IQP and its solute concentration reach maximum values. In Al-8.2 at % Mn alloy  $\dot{T}_0 \approx 2.4 \times 10^6$  K sec<sup>-1</sup>.

## References

1. D. SHECHTMAN, I. A. BLECH, D. GRATIAS and J. W. CAHN, *Phys. Rev. Lett.* **53** (1984) 1951.
2. F. H. SAMUEL, A. M. SAMUEL, A. de JONCKERE and F. GERIN, *Met. Trans. A* **17** (1986) 1671.
3. A. INOUE, L. ARNBERG, B. LEHTINEN, M. OGUCHI and T. MASUMOTO, *ibid.* **17** (1986) 1657.
4. C. SURYANARAYANA and H. JONES, *Int. J. Rapid Solid.* **3** (1987) 253.
5. S. M. ANLAGE and B. FULTZ, *J. Mater. Res.* **3** (1988) 421.
6. D. M. FOLLSTAEDT and J. A. KNAPP, *Mater. Sci. Engng.* **99** (1988) 367.
7. K. KIMURA, T. HASHIMOTO, K. SUZUKI, K. NAGASAWA, H. INO and S. TAKEUCHI, *J. Phys. Soc. Jpn.* **55** (1986) 534.
8. K. F. KELTON and J. C. HOLZER, *Mater. Sci. Engng.* **99** (1988) 389.
9. K. YU-ZHANG, M. HARMELIN, A. QUIVY, Y. CALVAYRAC, J. BIGET and R. PROTIER, *ibid.* **99** (1988) 385.
10. S. A. MYERS and C. C. KOCH, *J. Mater. Res.* **4** (1989) 44.
11. E. VOGT and G. FROMMEYER, *Z. Metallk.* **78** (1987) 262.
12. J. BARAM, *J. Mater. Sci.* **23** (1988) 405.
13. H. JONES, *Rep. Prog. Phys.* **36** (1973) 1425.
14. *Idem*, in "Rapid Solidification Processing I", edited by R. Mehrabian, B. H. Kear and M. Cohen (Claitor's, Baton Rouge, 1978).
15. R. A. DUNLAP and K. DILI, *J. Phys. F. Met. Phys.* **16** (1986) 11.
16. R. HULTGREN, R. L. ORR, P. D. ANDERSON and K. K. KELLEY, "Selected Values of Thermodynamic Properties of Binary Alloys" (ASM, Metals Park, 1973).
17. P. BAK, *Phys. Rev. Lett.* **54** (1985) 1417.
18. T. RAJASEKHARAN and J. A. SEKHAR, *Scripta Metall.* **20** (1986) 235.
19. H. P. KLUG and L. E. ALEXANDER, "X-ray Diffraction Procedures for Polycrystalline and Amorphous Materials", 2nd Edn (Wiley, New York, 1974).
20. S. P. BHAT, T. R. RAMACHANDRAN and A. K. JENA, *J. Mater. Sci.* **9** (1974) 1759.
21. CHENG TIANYI and ZHANG SHOUHYA, *Phys. B* **153** (1988) 209.
22. R. J. SCHAEFER, L. A. BENDERSKY and F. S. BIANCANELLO, *J. de Phys.* **C3** (1986) 311.
23. D. SHECHTMAN, R. J. SCHAEFER and F. S. BIANCANELLO, *Met. Trans. A* **15** (1984) 1987.
24. D. SHECHTMAN, *Mater. Sci. Forum* **22-24** (1987) 1.
25. CHENG TIANYI and ZHANG SHOUHYA, *J. Mater. Sci. Lett.* **9** (1990) 953.
26. *Idem*, "Rapid Solidification Technology and Advanced Alloys" (Aerospatial Publishing House, Beijing, 1990).
27. L. A. BENDERSKY and S. D. RIDDER, *J. Mater. Res.* **1** (1986) 405.
28. G. V. S. SASTRY, V. V. RAO, P. RAMACHANDRARAO and T. R. ANANTHARAMAN, *Scripta Metall.* **20** (1986) 191.

Received 21 August 1989  
and accepted 19 February 1990